

Status epilepticus-induced neuronal degeneration in the immature rat zona incerta is confined to its rostral sector

Azzat Al-Redouan^{1*}, Rastislav Druga^{1,2,3}, Martin Salaj¹, Hana Kubova²

¹ Department of Anatomy, Second Faculty of Medicine, Charles University, Prague, Czech Republic

² Department of Developmental Epileptology, Institute of Physiology, The Czech Academy of Sciences, Prague, Czech Republic

³ Department of Anatomy, First Faculty of Medicine, Charles University, Prague, Czech Republic

*Email: azzat.al-redouan@lfmotol.cuni.cz

The distribution and morphology of neuronal degeneration were observed and analyzed in each sector of the zona incerta in a lithium-pilocarpine (LiCl) Wistar rat model of status epilepticus in 12, 15, 18, 21, and 25-day-old rats and survival intervals of 4, 8, 12, 24, and 48 hours. Status epilepticus was induced *via* intraperitoneal (IP) injection of LiCl (3 mmol/kg) 24 hours before an injection of pilocarpine (40 mg/kg, IP). Motor seizures were suppressed by paraldehyde (0.3-0.6 ml/kg, IP) two hours after status epilepticus onset. Animals were anesthetized using urethane and perfused with phosphate-buffered saline followed by 4% paraformaldehyde. Brains were sectioned and Nissl stained for map guidance, with fluoro-Jade B fluorescence used to detect degenerated neurons. Fluoro-jade B-positive neurons were plotted to a standard stereotaxic atlas, their distribution was quantified, and their long-axis diameter was measured. Fluoro-jade B-positive neurons were found in pups aged 15 days and older 24 hours after status epilepticus, in which their numbers increased, and their perikaryon size decreased with advancing age. Thus, neuronal damage severity was dependent on age and survival interval. Neuronal damage was only found in the rostral sector of the zona incerta, a region that exhibits a small number of inhibitory neurons and is reciprocally connected to the limbic cortex. This system of hyperactivity, coupled with inhibitory neurons, may be the underlying cause of the neuronal degeneration and explain why it was confined to the rostral sector of the zona incerta.

Key words: zona incerta, epilepsy, seizure, degenerative neuronal changes

INTRODUCTION

The zona incerta (ZI) is a diencephalic nucleus that, together with the thalamic reticular and ventral lateral geniculate nuclei, has developmental origins with the ventral thalamus (Jones, 1985). Gene expression studies show that the ZI is part of prosomere-3, which gives rise to the development of the reticular nucleus of the thalamus, the ZI, and the pregeniculate nucleus (ventral lateral geniculate). Furthermore, GABAergic neurons prevail within prosomere-3 derivatives (Puelles & Ferran, 2012; Puelles et al., 2013).

The ZI in rats extends from the level of the paraventricular nucleus of the hypothalamus caudally to the rostral pole of the red nucleus. According to the Paxinos and Watson (2007) atlas, the ZI sits between -1.92 mm rostrally from bregma to -5.16 mm caudally from bregma. The ZI is in contact with the medial lemniscus and the subthalamic nucleus, which merge the ZI dorsally and ventrally.

Several studies showed that the mammalian ZI is a heterogeneous structure composed of several cytoarchitectonic sectors (Kolmac & Mitrofanis, 1999). In the rat, the ZI is divided into rostral (ZIR), dorsal (ZID), ventral (ZIV) and caudal (ZIC) sectors, with each com-

posed of different cytoarchitecture, immunocytochemical characteristics, and connectivity patterns (May et al., 1997; Kolmac & Mitrofanis, 1999; Mitrofanis & Mikuletic, 1999; Mitrofanis, 2005; Cavdar et al., 2006; Watson et al., 2014; 2015). The rat ZID and ZIV are located in the center of the ZI, and the ZIR and ZIC occupy the rostral and caudal poles of the nucleus, with the sectors defined by neurochemical and cytoarchitectonic markers. However, other immunohistochemical markers are distributed in most ZI sectors (Kolmac & Mitrofanis, 1999), with the ZIR containing neurons that express glutamate, somatostatin (SOM), nicotinamide adenine dinucleotide phosphate-diaphorase (NADPH-d), and tyrosine hydroxylase. Meanwhile, the ZID has glutamate, calretinin, and NADPH-d abundant neurons, with parvalbumin (PV) positive neurons in the medial part. The ZIV contains GABAergic neurons that co-express PV to some extent, while the ZIC includes some calbindin-positive neurons, although an acetylcholinesterase-positive neuropil was found in its caudal pole. In addition, a small number of neurofilament H non-phosphorylated (SMI-32) positive cells were reported in the ZID and ZIV (Watson et al., 2014).

Rat ZI projections are complex, extensive, and reciprocally organized in some structures and principally connect with the cerebral cortex, basal ganglia, diencephalon (thalamus and hypothalamus), brainstem, and spinal cord (Lin et al., 1990; 1997; Kolmac et al., 1998; Bartho et al., 2002; Guillery & Harting, 2003; Mitrofanis, 2005; Cavdar et al., 2006). An important feature of ZI connectivity is the interconnections between discrete regions. Neurons in one area may influence the activity of ipsilateral neurons and corresponding and non-corresponding contralateral ZI sectors (Power et al., 1999; Power & Mitrofanis, 1999a; 1999b).

The complex connectivity of the ZI exhibits widespread afferent and efferent projections, with many centers of neuraxis. This complexity, together with its immunocytochemical heterogeneity, is closely related to its diverse functions in somatosensory and nociceptive processing, drinking and feeding, sexual behavior, motor activities, arousal, and attention (Roger & Cadusseau, 1985; Kolmac & Mitrofanis, 1999). Functionally, the ZI is associated with motor coordination, sensory processing, visuomotor integration, cortical activation, vigilance regulation, and several behaviors. The ZI also forms part of the arousal network circuit and is associated with attention. ZI Stimulation generates locomotor activity, namely limbic-related movements. Several studies demonstrated that the ZI influences visceral activity, including cardiovascular functions, digestion, and sexual cycles (Mitrofanis, 2005; Kita et al., 2014; Ossowska, 2020; Wang et al., 2020).

Generalized tonic-clonic seizures are triggered by microinjection of cholinergic agonists into the ZI of adult rats (Mello et al., 1993; Brudzynski et al., 1995), meaning that the ZI is a sensitive structure in experimentally induced seizures. Later, it was found that manipulating the GABAergic system of the ZI led to seizure activity modulation (Brudzynski et al., 1995; Hamani et al., 2002). ZI administration of the GABAA agonist muscimol demonstrated a pro-convulsant effect in the pilocarpine epilepsy model in adult rats, while the GABA, antagonist bicuculline had anticonvulsant (Turski et al., 1991; Hamani et al., 2002) and paradoxical effects (Mares et al., 2000; Johnston, 2013). Not all ionotropic GABA receptors are susceptible to bicuculline, and not all ionotropic GABA receptors antagonists are convulsants (Johnston, 2013). On the contrary, high doses of bicuculline caused generalized seizures in 12-day-old and younger pups (Mares et al.,

The ZIC recently became a target for deep brain stimulation procedures used to treat Parkinson's disease symptoms (Watson et al., 2015; Jochim et al., 2016; Ossowska, 2020).

In a series of previously published articles, we demonstrated that LiCl induced status epilepticus (SE) in immature rats and caused severe neuronal degeneration in several thalamic nuclei. Degeneration was noticed in 12-day-old animals and progressed to one week after SE (Kubova et al., 2002; 2005; Druga et al., 2005). Similar findings also showed severely damaged thalamic nuclei in adult rats after SE induced by pilocarpine and kainic acid administration in a study by Covolan and Mello (2000). Neuronal injury was also reported in the ZI after SE in adult rats, with a moderate number of damaged argyrophilic neurons found in this nucleus at longer survival intervals (8, 24, and 48 hours) in a pilocarpine and kainic acid model of temporal lobe epilepsy (Covolan & Mello, 2000). However, data relating to ZI damage in immature rats during postnatal development are lacking in the literature.

The study aimed to investigate whether LiCl-induced SE results in neuronal damage in the ZI of immature rats. Another goal was to assess the distribution and dynamics of neuronal degeneration and the morphology of degenerated neurons within the individual sectors of the ZI during postnatal development.

METHODS

Animal care and experimental procedures were conducted in accordance with European Community Council Directives 86/609 EEC. The Animal Care and Use Committee of the Institute of Physiology of the

Academy of Sciences of the Czech Republic approved the experiments.

The study and access to specimens was approved for research and education purposes by the Institutional Review Board (IRB) - The Ethics Committee of the University Hospital Motol and Second Faculty of Medicine, Charles University, Prague, Czech Republic (Reference ID no. EK-1175.1.19/22).

Experimental procedure

The experiment employed the LiCl model of SE (Handforth & Treiman, 1995) in 125 Wistar rat pups aged 12 (P12), 15 (P15), 18 (P18), 21 (P21), and 25 (P25) days old, with 25 animals per age group divided into five per survival intervals of 4, 8, 12, 24, and 48 hours. Each age and interval group contained five rats (four experimental and one control). The sample consisted of the animals that developed seizures and were included in the study. Only animals exhibiting convulsive SE were included, with 42 excluded as they did not develop severe observable motor seizure activity, and three excluded due to dying during SE.

To induce SE, LiCl (3 mmol/kg) was injected intraperitoneally (IP) 24 hours before pilocarpine (40 mg/kg, IP). Control animals were treated with LiCl and saline. Two hours after SE onset, motor seizures were suppressed with 0.3 ml/kg paraldehyde IP in P12, P15, and P18 rats and 0.6 ml/kg IP in P21 and P25 animals.

Animals were deeply anesthetized with 20% urethane (2.5 g/kg, IP) and perfused at room temperature with phosphate-buffered saline (PBS) followed by 4% paraformaldehyde mixed in 0.1 M PBS (pH 7.4, 4°C). Brains were removed from the skull, fixed for three hours, divided into blocks and cryoprotected in 30% sucrose. The brain blocks were sectioned (50 μm) in the coronal plane and stained in alternating sections with cresyl violet to provide map guidance and fluoro-Jade B (FJB) to detect damaged neurons (Schmued & Hopkins, 2000).

Control animals of all age and time groups were treated with equal volumes of LiCl, but the pilocarpine solution was replaced with saline. Paraldehyde was administered two hours after the saline injection at a corresponding dose.

Brain sections throughout the entire rostrocaudal extent of the brain were examined. An Olympus BX51 fluorescent microscope equipped with an Olympus DP72 digital camera and QuickPHOTO Micro 32 software was used to outline the ZI and its subdivisions and count the FJB-positive neurons. Images were sharpened and converted to black and white to improve the cell-to-background contrast.

FJB-labeled degenerated neurons were plotted and transferred to standard stereotaxic rat brain sections where the ZI resides using the MDPlot $^{\rm m}$ 5.1 computer-aided digitizing system (Accustage, MN, USA) for plotting and CorrelDraw software (version 11) for illustration.

Lesion evaluation

The semi-quantitative analysis was achieved by localizing and counting the FJB-positive neurons in the observed ZI in four sections per animal from the 24-hour post-SE survival intervals (Table 1).

The morphological qualitative data was obtained objectively by measuring the perikaryon long-axis diameter of 50 cells per age/survival interval (Table 1).

Statistical analysis

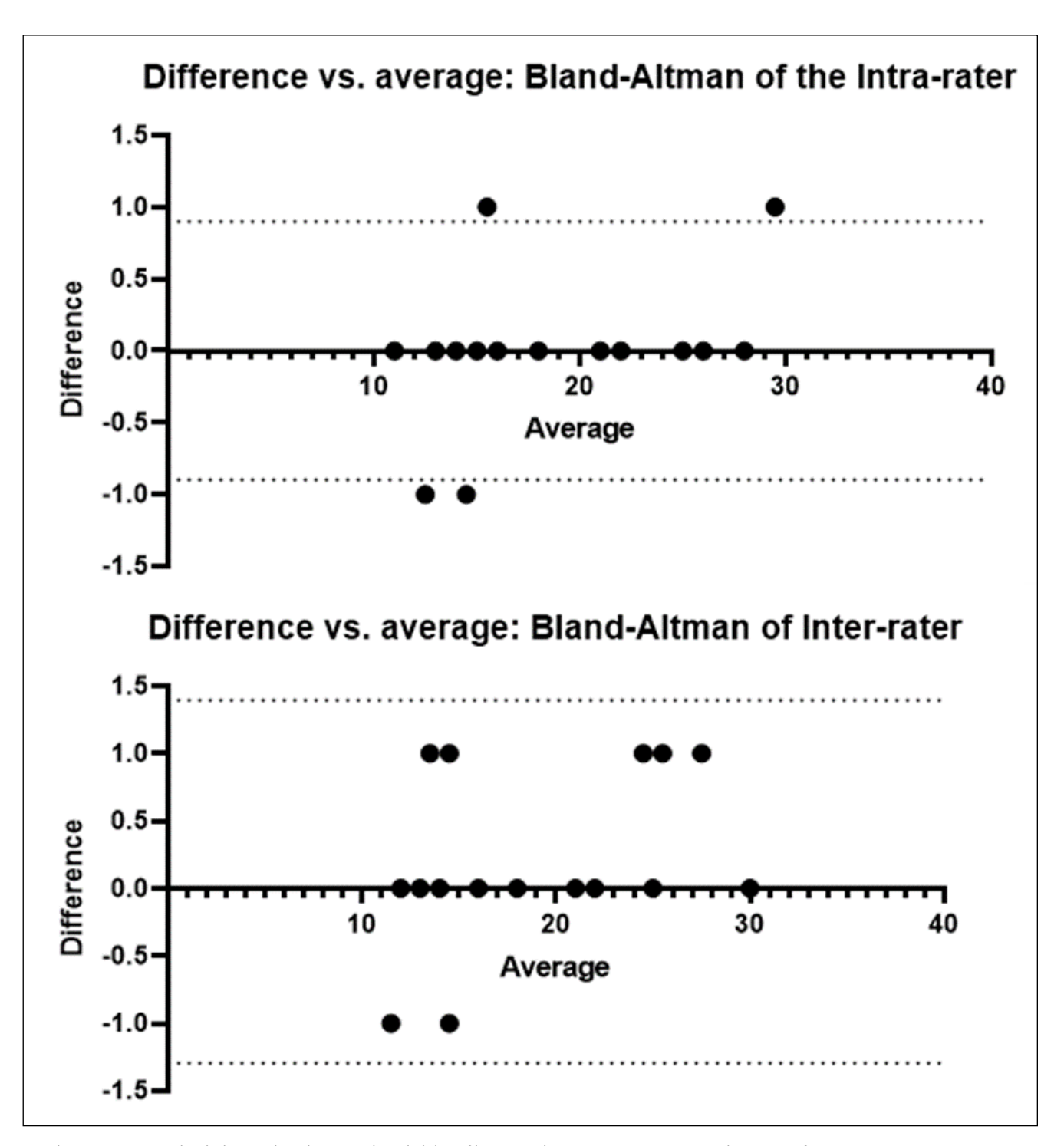
Data analysis employed Microsoft Excel, Arcus Quickstat Biomedical 1.1, and GraphPad (version 9.1.2.226). The reliability of data collection was assessed using eight samples for cell counting of FJB-positive neurons and 20 samples for measuring perikaryon long-axis diameter. The data were independently collected by two observers one week apart to reduce

Table 1. Perikaryon long-axis diameter (μm) of fluoro-jade B-positive neurons in P15, P18, P21, and P25 age groups 24 hours after status epilepticus.

Age/survival interval group	Fluoro-jade B-positive neurons	Long-axis diameter (μm)			
		Min	Median	Max	± SD
15/24	56	11	19.5	34	5.45
18/24	116	13	20.5	30	4.72
21/24	147	11	16.0	29	5.34
25/24	163	11	13.0	22	3.21

confirmation bias. The inter- and intra-rater reliability was evaluated by linear regression, and the limits of agreement and bias were plotted using Bland-Altman plots (Supplementary Fig. 1).

A non-normal data distribution was confirmed by the Shapiro-Wilk test, while the Kruskal-Wallis test determined the significance of differences in FJB-positive neuron profiles. Subsequently, post hoc Dunn's tests compared the significance of differences between the age groups that contained FJB-positive neurons in the 24-hour post-SE survival interval (Supplementary material).



 $Supplementary Fig.~1.~Bland-Altman~plots~depicting~the~reliability~of~long-axis~diameter~measurements~with~a~range~of~\pm~1.0~\mu m.$

RESULTS

Degenerated neuron detection

All FJB-positive neurons were confined bilaterally in the ZIR of both hemispheres, as shown in Fig. 1. The number of FJB-positive neurons increased with age, as shown in Table 1.

No FJB-positive neurons were found in the ZI at any survival interval in 12-day-old animals group.

In 15-day-old animals, the ZI contained only isolated FJB-positive neurons in two out of four animals in the 24-hour survival group. Degenerating FJB-positive neurons were found in two brain sections and were distributed in the ZIR of both hemispheres, though they were confined to the periphery (Fig. 2).

In 18-day-old animals, the ZI contained a moderate number of degenerated neurons (Table 1), which was 53.40% higher than in the P15 age group. FJB-positivity was found in the ZIR of five to six brain sections, while the other sectors did not contain any FJB-positive neurons. The neuronal damage was distributed without clustering over the central and medial aspects of the ZIR in the 24-hour survival group (Fig. 2).

In 21 and 25-day-old animals, the ZI contained more degenerated neurons in these two age groups (Table 1). The P21 group had 19.20% more degenerated neurons than the P18 group and 11.00% fewer than the P25 group. Similar to the P18 group, the damage was confined to the ZIR and found in five brain sections (Fig. 1). There were no FJB-positive neurons detected in the ZIV, ZID, or ZIC in all cases and survival intervals. The lesion was localized centrally in the ZIR, with increased clustering in the P25 24-hour survival group (Fig. 2).

In control animals, FJB-positive neurons were not detected in any of the control animals.

Somatodendritic characteristics of degenerated neurons

The perikarya long-axis diameters are listed by age groups in Table 1.

In the shorter (≤24 hours) intervals after SE, the FJB-positive neurons exhibited intense staining of the cell body and proximal dendrites. In the longer survival intervals (24 and 48 hours), the ZIR exhibited a mixture of intensely and less intensely stained neuronal bodies that were frequently shrunken, as indicated by a decrease in their long-axis. Additionally, small stained particles had formed, which were probably caused by disintegrated axons, axon terminals, and peripheral dendritic branches. The particles are respon-

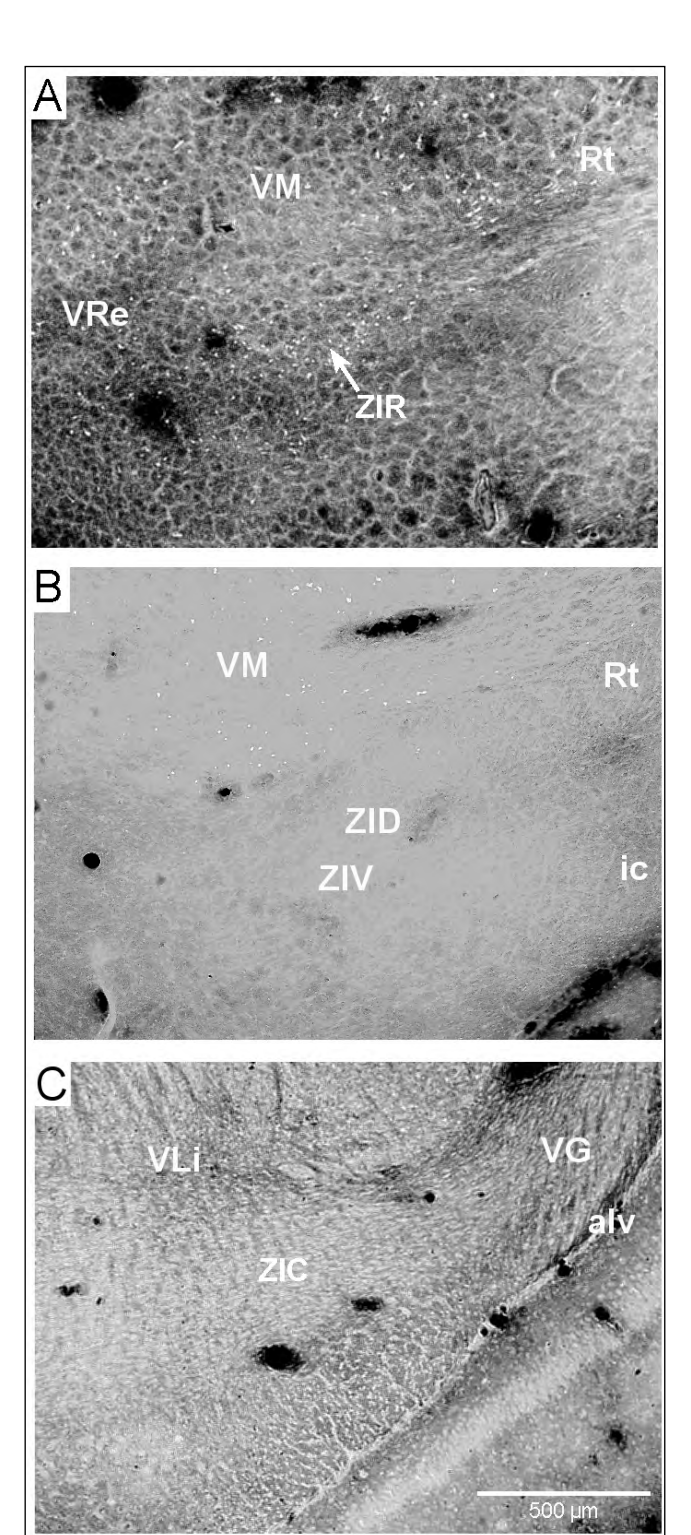


Fig. 1. Fluorescent microscopic photomicrograph showing fluoro-jade B-positive neurons in the left hemisphere of P25 rats 24 hours post-status epilepticus. (A) Rostral sector of the zona incerta. (B) Middle sectors of the zona incerta comprising the ventral and dorsal sectors. (C) Caudal sector of the zona incerta. ZIC: caudal zona incerta; ZID: dorsal zona incerta; ZIR: rostral zona incerta; ZIV: ventral zona incerta.

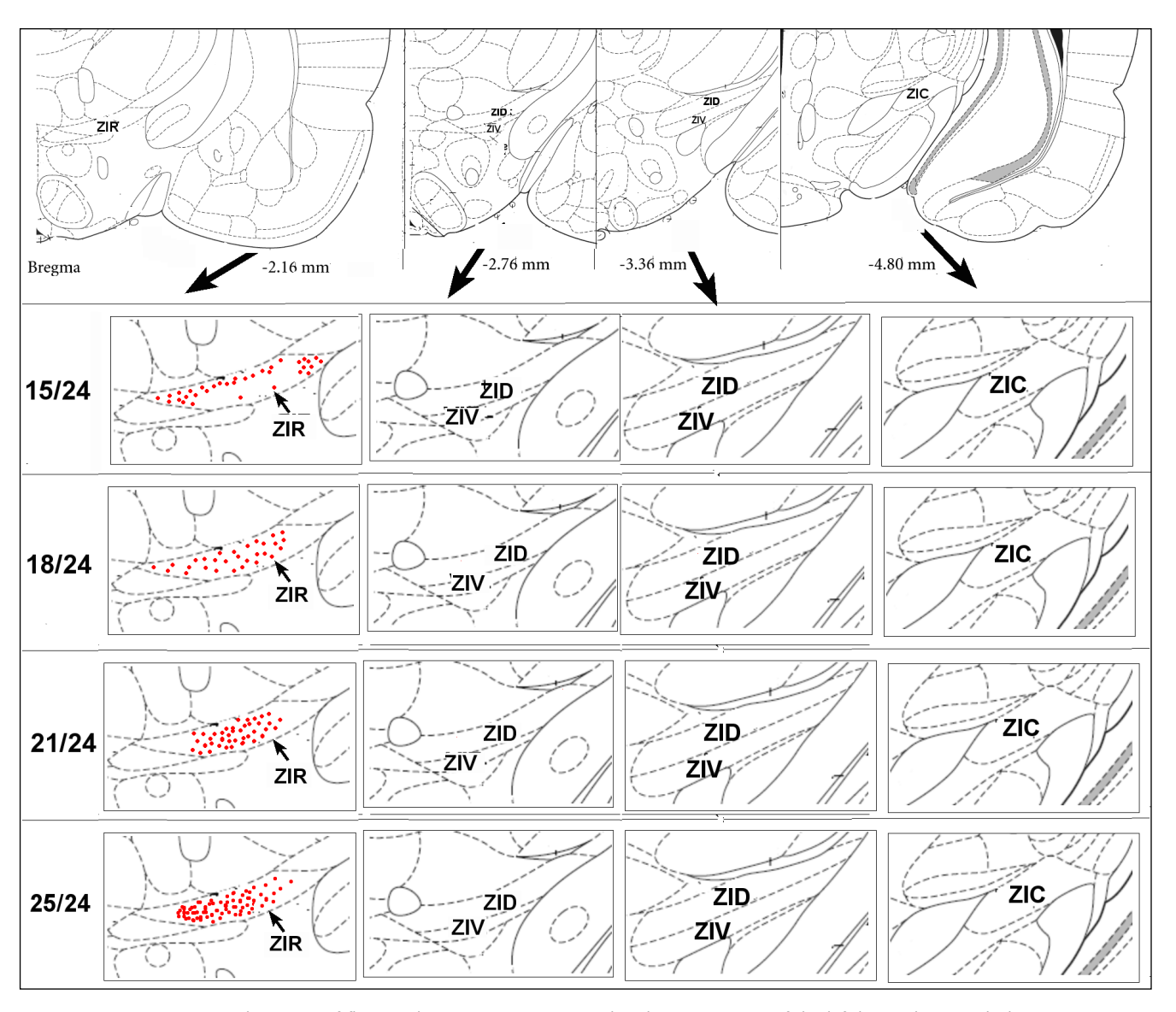


Fig. 2. Representative coronal sections of fluoro-jade B-positive neurons within the zona incerta of the left hemisphere. Each dot represents one FJB-positive neuron. The number below each section refers to the distance from bregma. The number before each row represents the age interval by days and the survival interval of 24 hours after status epilepticus. ZIC: caudal zona incerta; ZID: dorsal zona incerta; ZIR: rostral zona incerta; ZIV: ventral zona incerta.

sible for the dusty appearance of the ZIR background shown in Fig. 3.

There was a noticeable change in cell morphology, with a gradual diminishing of the perikaryon long-axis diameters as animal age increased. The average perikaryon long-axis diameter in the ZI of control rat brain sections was 40 μ m and was lower by 49.40% in P15, 49.90% in P18, 52.45% in P21, and 65.20% in P25 animals. Such reductions indicate an age-dependent pattern of lesion severity, which was most prominently evident at the 24-hour post-SE survival interval (Table 1 and Fig. 4).

The statistical analyses showed significant differences between the 15, 18, 21, and 25-day age groups at the 24-hour post-SE survival interval, with p-values of <0.0001 between all four groups (Supplementary material).

DISCUSSION

The presented data provide evidence that LiCl-induced SE caused neuronal degeneration within the ZI of both hemispheres in immature rats and that damage

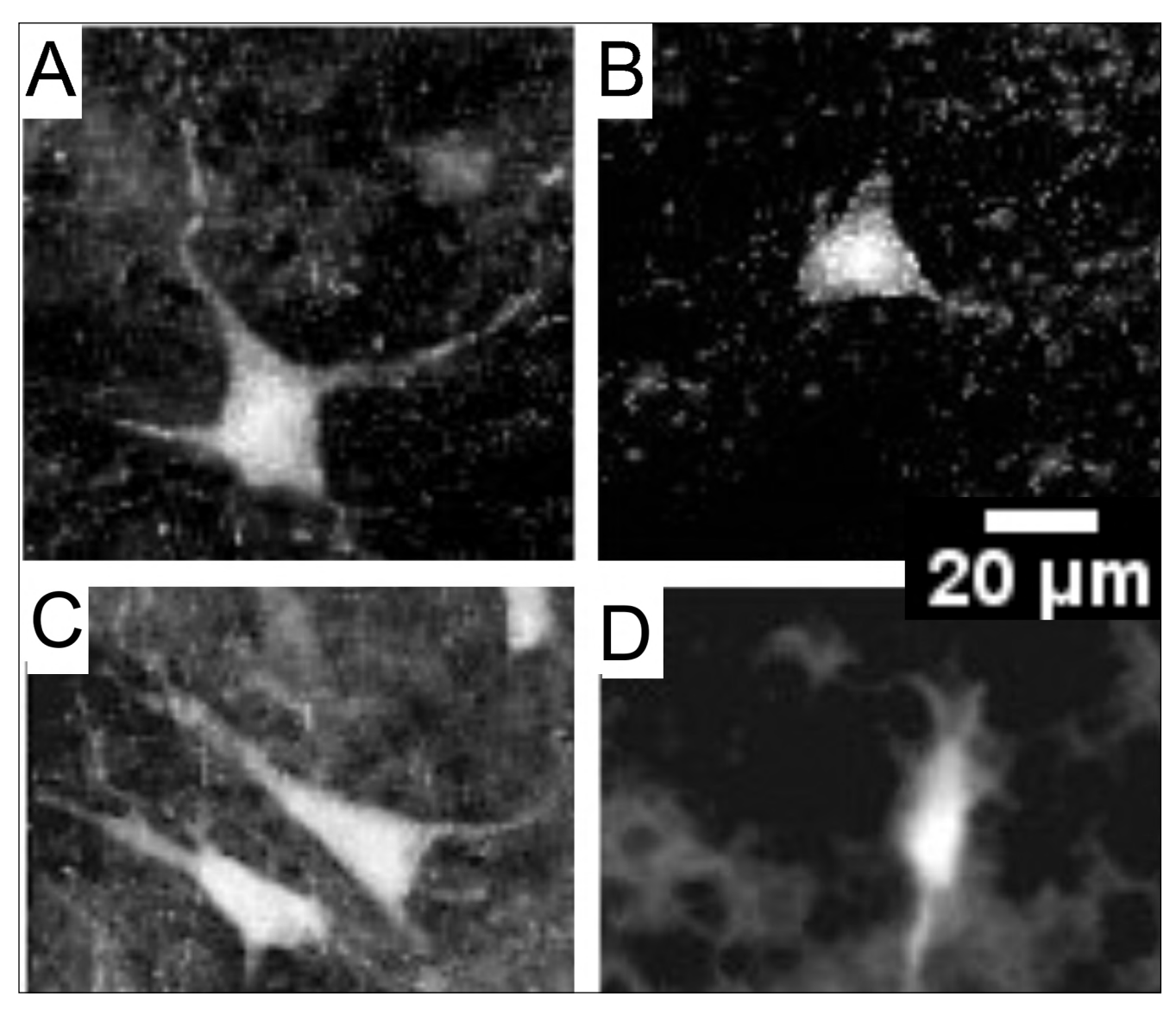


Fig. 3. Fluorescent microscopic (45x objective magnification) photomicrograph showing fluoro-jade B-positive neurons at 24 hours post-status epilepticus for all age intervals. (A) P15. (B) P18. (C) P21. (D) P25.

severity correlated with age. We found an increase in damage severity by age interval, as indicated by the decrease in perikarya long-axis diameters. There were no FJB-positive neurons in any ZI sectors in P12 rats across all their survival intervals. However, SE-induced neuronal degeneration within the ZI was observed in P15, P18, P21, and P25 animals. The neuronal degeneration was restricted to the ZIR since the ZIV, ZID, and ZIC did not exhibit any neuronal degeneration.

Several studies investigated extra-hippocampal neuronal damage in the immature rat using the LiCl model of SE (Cavalheiro et al., 1987; Hirsch et al., 1992; Priel et al., 1996; Sankar et al., 1997; 1998; Kubova et al., 2001; Dube et al., 2001; Roch et al., 2002; Mares et al., 2005; Nairismagi et al., 2006). Based on our knowledge of the current literature, SE-induced neuronal damage in the ZI has not been reported. However, a previous study by Scholl et al. (2013) showed some FJB-positive cells in the ZI, though no details were provided regarding their distribution within ZI sectors.

The available literature is limited and does not provide evidence that could explain the neural degeneration observed in the ZIR in the current study. Furthermore, data derived from combined morphological, electrophysiological, and neurochemical studies on ZI neurons and ZI neuronal microcircuits are lacking. Indeed, the neurochemical properties of ZI neurons were only described in studies by Kolmac and Mitrofamis (1999)

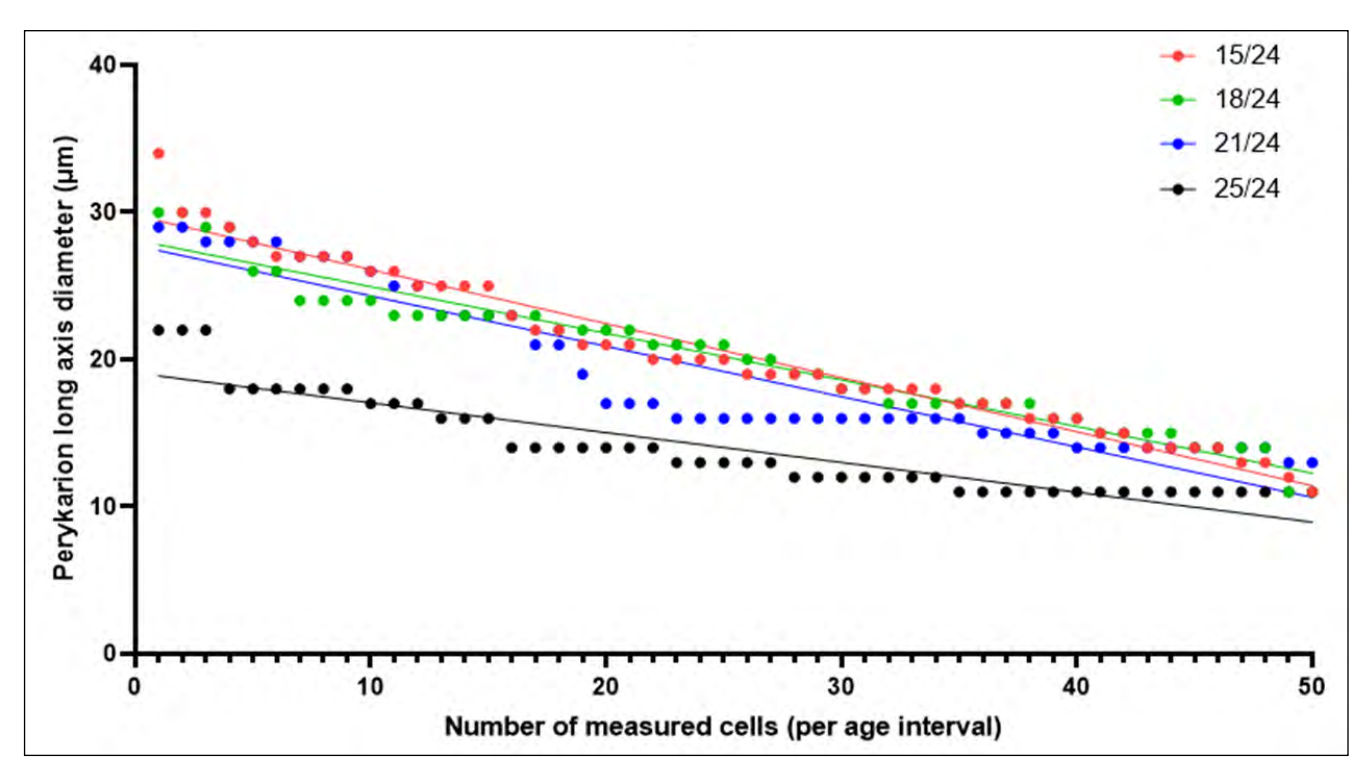


Fig. 4. Fluoro-jade B-positive neuron long-axis diameter (μ m) measured in 50 cells per age interval. Perikaryon long-axis diameter (μ m), with p<0.05 indicating a decrease in size that correlated to increased severity by age.

and Mitrofamis (2005). Nonetheless, animal models can provide promising insights into and expand our understanding of these neuronal mechanisms (Becker, 2018; Thom, 2018). However, our study was confined to convulsive epileptic seizures, unlike the study by Vila Verde et al. (2021) on focal non-convulsive SE.

Neuronal damage peaked in 15-day-old rats, with a gradual increase in damage severity through the older age groups demonstrated by differing populations of perikarya counts and characteristics. The number increased between P15 and P21 at a higher rate than in the P25 adult-aged rats. The perikarya size (expressed in long-axis diameter) shrunk at a relatively slower rate between 15 and 21 days (P15-P21) and was more markedly reduced in 25-day-old animals (P25) (Table 1 and Fig. 4). The age dependency was observed in other structures, such as the thalamus, in a previous study by Druga et al. (2005).

The distribution of damaged neurons was similar in P18 and P21, where it was scattered among the central area of the ZIR, though it was confined to the periphery of the ZIR in P15 rats. Damage was also confined centrally in P25 rats, but the pattern was clustered, indicating confocal damage in the center of the ZIR. Multipolar cells were only discernible in P15 and were not seen in the older animals, indicating an increased

loss of dendritic connectivity by age. Damage severity peaking in adult animals was reported in other studies addressing differing brain areas (Cavalheiro et al., 1987; Hirsch et al., 1992; Priel et al., 1996; Sankar et al., 1997; 1998; Kubova et al., 2001; Dube et al., 2001; Roch et al., 2002; Mares et al., 2005; Nairismagi et al., 2006).

Morphological mechanisms of the neuronal lesion

One possible mechanism responsible for the neuronal damage within the ZIR is the hyperactivity of the excitatory glutamatergic fiber system associated with glutamate excitotoxicity. The cortical afferent projection that terminates in the ZIR could be involved in this excitotoxicity. Indeed, substantial cortical projections into the ZIR arising from the cingulate cortical area (Mitrofanis & Mikuletic, 1999; Cavdar et al., 2006) are thought to belong to the glutamatergic excitatory system.

According to several immunochemical studies, numerous neurochemical markers are expressed differently in ZI subdivisions (Nicolelis, 1992; 1995; Wagner et al., 1995; Kolmac & Mitrofanis, 1999; Scholl et al., 2013). The ZIV contains abundant GABA, glutamic acid decarboxylase (GAD), and PV-expressing neurons,

comprising more than 80% of the total cells, characteristic of inhibitory neurons. Furthermore, the ZIV contains the largest percentage (95%) of PV-positive neurons. Most inhibitory neurons in the ZIV could protect the region and, therefore, may explain the lack of FJB-positive neurons found in our experiments. Nevertheless, 20-25% of GABA and GAD and around 10% of PV-expressing neurons were located in the ZID. On the other hand, 50% of ZIC neurons are NADPH-positive, and 15% are SOM-positive (Kolmac & Mitrofanis, 1999). Although the density of inhibitory neurons within the ZID is lower than the ZIV (Kolmac & Mitrofanis, 1999), they could be sufficient to suppress excitotoxic hyperactivities and consecutive neuronal damage in this ZI subdivision.

The rostral sector of the zona incerta is vulnerable to status epilepticus

The ZIR is a heterogeneous structure containing glutamatergic, GABAergic, dopaminergic, and SOM-positive neurons, but the density of their neurochemically defined cells is low to moderate, the GABAergic and PV neurons representing about 10% of the cell population (Mitrofanis, 2005). According to Kolmac and Mitrofanis (1999), tyrosine hydroxylase immunoreactive cells were found almost exclusively within the ZIR, forming about 15% of the cells, and probably represent part of the dopaminergic system designated as group A-13. However, the cellular mechanisms activated by dopamine in the ZIR are still obscure. The neuropeptide SOM was demonstrated in the ZIR (around 35% of cells) but was lower in the ZIV and ZID (25% and 15% of cells, respectively). The role of SOM neurons in the neocortical circuits is a recent subject of research focus, with several articles stating that SOM interneurons robustly inhibit PV interneurons and enhance the activity of pyramidal neurons. The aforementioned circuit can ultimately influence various types of behavior, including neuronal excitotoxicity potentiation (Xu et al., 2019), though the existence of inhibitory circuits in the ZIR is unconfirmed.

According to Steinert et al. (2010), most NADPH-d-positive neurons are found in the ZID (40% of cells) and the ZIR (15% of cells), and it is broadly understood that neuronal nitric oxide synthase (NOS) contributes to a variety of neurodegenerative processes accompanied with neurotoxicity. In addition to the above-mentioned substances, the ZIR contains a small number of serotonin-releasing neurons (5%) and glutamate-positive neurons (15%) (Steinert et al., 2010).

There is a very low density of inhibitory GABAergic neurons within the ZIR that are visualized by several markers (GABA, GAD, and PV). As such, the weak inhibitory nature of the ZIR, accompanied by other neuroactive substances (SOM and NOS), might be the underlying cause of the vulnerability of this ZI sector to neuronal damage after SE.

Since this was a morphological study of post-mortem damage to the ZI, the consequence of damage within the ZIR on its function in pathological states could not be tested. Furthermore, an inhibitory agent, such as methylscopolamine, was not administered in our LiCl model, as suggested by others (Ahmed Juvale & Che Has, 2020), since it can block seizures.

CONCLUSIONS

The study provides evidence that LiCl-induced SE provoked neuronal damage in the ZI, although FJB-positive neurons were not detected in the ZI of the 12-day-old pups and contained a low number of degenerated neurons in the 15-day-old pups. However, a moderate number of degenerated neurons were found in the ZI of older animals. As such, neuronal damage severity was dependent on age and survival interval. Furthermore, degenerated neurons within the ZI were restricted to its rostral area.

ACKNOWLEDGMENTS

This research was supported by the project National Institute for Neurology Research (Programme EXCE-LES, ID Project NO. LX22NPO5107); Funded by the European Union – Next Generation EU. The study was also funded by the Grant Agency of Czech Republic (GAČR), project No. 23-05274S, and support for long-term conceptual development of research organization RVO: 67985823.

REFERENCES

Ahmed Juvale, I. I., & Che Has, A. T. (2020). The evolution of the pilocarpine animal model of status epilepticus. *Heliyon*, *6*(7), e04557. https://doi.org/10.1016/j.heliyon.2020.e04557

Barthó, P., Freund, T. F., & Acsády, L. (2002). Selective GABAergic innervation of thalamic nuclei from zona incerta. *The European journal of neuroscience*, *16*(6), 999–1014. https://doi.org/10.1046/j.1460-9568.2002.02157.x Becker A. J. (2018). Review: Animal models of acquired epilepsy: insights into mechanisms of human epileptogenesis. *Neuropathology and applied neurobiology*, *44*(1), 112–129. https://doi.org/10.1111/nan.12451 Brudzynski, S. M., Cruickshank, J. W., & McLachlan, R. S. (1995). Cholinergic mechanisms in generalized seizures: importance of the zona incerta.

- The Canadian journal of neurological sciences, 22(2), 116–120. https://doi.org/10.1017/s031716710004018x
- Cavalheiro, E. A., Silva, D. F., Turski, W. A., Calderazzo-Filho, L. S., Bortolotto, Z. A., & Turski, L. (1987). The susceptibility of rats to pilocarpine-induced seizures is age-dependent. *Brain research*, 465(1-2), 43–58. https://doi.org/10.1016/0165-3806(87)90227-6
- Cavdar, S., Onat, F., Cakmak, Y. O., Saka, E., Yananli, H. R., & Aker, R. (2006). Connections of the zona incerta to the reticular nucleus of the thalamus in the rat. *Journal of anatomy*, 209(2), 251–258. https://doi.org/10.1111/j.1469-7580.2006.00600.x
- Covolan, L., & Mello, L. E. (2000). Temporal profile of neuronal injury following pilocarpine or kainic acid-induced status epilepticus. *Epilepsy research*, 39(2), 133–152. https://doi.org/10.1016/s0920-1211(99)00119-9
- Druga, R., Mares, P., Otáhal, J., & Kubová, H. (2005). Degenerative neuronal changes in the rat thalamus induced by status epilepticus at different developmental stages. *Epilepsy research*, 63(1), 43–65. https://doi.org/ 10.1016/j.eplepsyres.2004.11.001
- Dubé, C., Boyet, S., Marescaux, C., & Nehlig, A. (2001). Relationship between neuronal loss and interictal glucose metabolism during the chronic phase of the lithium-pilocarpine model of epilepsy in the immature and adult rat. *Experimental neurology*, 167(2), 227–241. https://doi.org/ 10.1006/exnr.2000.7561
- Guillery, R. W., & Harting, J. K. (2003). Structure and connections of the thalamic reticular nucleus: Advancing views over half a century. *The Jour-nal of comparative neurology*, 463(4), 360–371. https://doi.org/10.1002/cne.10738
- Hamani, C., Sakabe, S., Bortolotto, Z. A., Cavalheiro, E. A., & Mello, L. E. (2002). Inhibitory role of the zona incerta in the pilocarpine model of epilepsy. *Epilepsy research*, 49(1), 73–80. https://doi.org/10.1016/ s0920-1211(02)00017-7
- Handforth, A., & Treiman, D. M. (1995). Functional mapping of the late stages of status epilepticus in the lithium-pilocarpine model in rat: a 14C-2-de-oxyglucose study. *Neuroscience*, *64*(4), 1075–1089. https://doi.org/10.1016/0306-4522(94)00377-h
- Hirsch, E., Baram, T. Z., & Snead, O. C., 3rd (1992). Ontogenic study of lithium-pilocarpine-induced status epilepticus in rats. *Brain research*, 583(1-2), 120–126. https://doi.org/10.1016/s0006-8993(10)80015-0
- Jochim, A., Gempt, J., Deschauer, M., Bernkopf, K., Schwarz, J., Kirschke, J. S., & Haslinger, B. (2016). Status Epilepticus After Subthalamic Deep Brain Stimulation Surgery in a Patient with Parkinson's Disease. World neurosurgery, 96, 614.e1-614.e6. https://doi.org/10.1016/j.wneu.2016.08.067
- Jones J. L. (1985). Neurophysiology. Basal facts, 7(2), 121–125.
- Johnston G. A. (2013). Advantages of an antagonist: bicuculline and other GABA antagonists. *British journal of pharmacology, 169*(2), 328–336. https://doi.org/10.1111/bph.12127
- Kita, T., Osten, P., & Kita, H. (2014). Rat subthalamic nucleus and zona incerta share extensively overlapped representations of cortical functional territories. *The Journal of comparative neurology*, *522*(18), 4043–4056. https://doi.org/10.1002/cne.23655
- Kolmac, C., & Mitrofanis, J. (1999). Distribution of various neurochemicals within the zona incerta: an immunocytochemical and histochemical study. *Anatomy and embryology*, 199(3), 265–280. https://doi.org/10.1007/s004290050227
- Kolmac, C. I., Power, B. D., & Mitrofanis, J. (1998). Patterns of connections between zona incerta and brainstem in rats. *The Journal of comparative neurology*, 396(4), 544–555. https://doi.org/10.1002/(sici)1096-9861 (19980713)396:4<544::aid-cne10>3.0.co;2-g
- Kubová, H., Druga, R., Haugvicová, R., Suchomelová, L., & Pitkanen, A. (2002). Dynamic changes of status epilepticus-induced neuronal degeneration in the mediodorsal nucleus of the thalamus during postnatal development of the rat. *Epilepsia*, 43 Suppl 5, 54–60. https://doi.org/10.1046/j.1528-1157.43.s.5.36.x

- Kubová, H., Druga, R., Lukasiuk, K., Suchomelová, L., Haugvicová, R., Jirmanová, I., & Pitkänen, A. (2001). Status epilepticus causes necrotic damage in the mediodorsal nucleus of the thalamus in immature rats. The Journal of neuroscience: the official journal of the Society for Neuroscience, 21(10), 3593–3599. https://doi.org/10.1523/ JNEUROSCI.21-10-03593.2001
- Kubová, H., Rejchrtová, J., Redkozubova, O., & Mares, P. (2005). Outcome of status epilepticus in immature rats varies according to the paraldehyde treatment. *Epilepsia*, *46 Suppl 5*, 38–42. https://doi.org/10.1111/j.1528-1167.2005.01005.x
- Lin, C. S., Nicolelis, M. A., Schneider, J. S., & Chapin, J. K. (1990). A major direct GABAergic pathway from zona incerta to neocortex. *Science (New York, N.Y.)*, 248(4962), 1553–1556. https://doi.org/10.1126/science.2360049
- Lin, R. C., Nicolelis, M. A., & Chapin, J. K. (1997). Topographic and laminar organizations of the incertocortical pathway in rats. *Neuroscience*, 81(3), 641–651. https://doi.org/10.1016/s0306-4522(97)00094-8
- Mares, P., Chino, M., Kubová, H., Mathern, P., & Veliký, M. (2000). Convulsant action of systemically administered glutamate and bicuculline methiodide in immature rats. *Epilepsy research*, *42*(2-3), 183–189. https://doi.org/10.1016/s0920-1211(00)00179-0
- Mares, P., Tsenov, G., Aleksakhina, K., Druga, R., & Kubová, H. (2005). Changes of cortical interhemispheric responses after status epilepticus in immature rats. *Epilepsia*, *46 Suppl 5*, 31–37. https://doi.org/10.1111/j.1528-1167.2005.01004.x
- May, P. J., Sun, W., & Hall, W. C. (1997). Reciprocal connections between the zona incerta and the pretectum and superior colliculus of the cat. *Neuroscience*, 77(4), 1091–1114. https://doi.org/10.1016/s0306-4522(96)00535-0
- Mello, L. E., Cavalheiro, E. A., Tan, A. M., Kupfer, W. R., Pretorius, J. K., Babb, T. L., & Finch, D. M. (1993). Circuit mechanisms of seizures in the pilocarpine model of chronic epilepsy: cell loss and mossy fiber sprouting. *Epilepsia*, 34(6), 985–995. https://doi.org/10.1111/j.1528-1157.1993. tb02123.x
- Mitrofanis, J., & Mikuletic, L. (1999). Organisation of the cortical projection to the zona incerta of the thalamus. *The Journal of comparative neurology*, 412(1), 173–185.
- Mitrofanis J. (2005). Some certainty for the "zone of uncertainty"? Exploring the function of the zona incerta. *Neuroscience*, *130*(1), 1–15. https://doi.org/10.1016/j.neuroscience.2004.08.017
- Nairismägi, J., Pitkänen, A., Kettunen, M. I., Kauppinen, R. A., & Kubova, H. (2006). Status epilepticus in 12-day-old rats leads to temporal lobe neurodegeneration and volume reduction: a histologic and MRI study. *Epilepsia*, 47(3), 479–488. https://doi.org/10.1111/j.1528-1167.2006.00455.x
- Nicolelis, M. A., Chapin, J. K., & Lin, R. C. (1995). Development of direct GABAergic projections from the zona incerta to the somatosensory cortex of the rat. *Neuroscience*, *65*(2), 609–631. https://doi.org/10.1016/0306-4522(94)00493-o
- Nicolelis, M. A., Chapin, J. K., & Lin, R. C. (1992). Somatotopic maps within the zona incerta relay parallel GABAergic somatosensory pathways to the neocortex, superior colliculus, and brainstem. *Brain research*, *577*(1), 134–141. https://doi.org/10.1016/0006-8993(92)90546-I
- Ossowska, K. (2020). Zona incerta as a therapeutic target in Parkinson's disease. *Journal of neurology*, 267(3), 591–606. https://doi.org/10.1007/s00415-019-09486-8
- Paxinos, G., Watson, C. (1997). The rat brain in stereotaxic coordinates. 3rd Ed. Acad. Press.
- Power, B. D., Kolmac, C. I., & Mitrofanis, J. (1999). Evidence for a large projection from the zona incerta to the dorsal thalamus. *The Journal of comparative neurology*, 404(4), 554–565.
- Power, B. D., & Mitrofanis, J. (1999a). Evidence for extensive inter-connections within the zona incerta in rats. *Neuroscience letters*, *267*(1), 9–12. https://doi.org/10.1016/s0304-3940(99)00313-4

- Power, B. D., & Mitrofanis, J. (1999b). Specificity of projection among cells of the zona incerta. *Journal of neurocytology*, *28*(6), 481–493. https://doi.org/10.1023/a: 1007005105679
- Priel, M. R., dos Santos, N. F., & Cavalheiro, E. A. (1996). Developmental aspects of the pilocarpine model of epilepsy. *Epilepsy research*, *26*(1), 115–121. https://doi.org/10.1016/s0920-1211(96)00047-2
- Puelles, L., & Ferran, J. L. (2012). Concept of neural genoarchitecture and its genomic fundament. *Frontiers in neuroanatomy*, *6*, 47. https://doi.org/10.3389/fnana.2012.00047
- Puelles, L., Harrison, M., Paxinos, G., & Watson, C. (2013). A developmental ontology for the mammalian brain based on the prosomeric model. *Trends in neurosciences*, *36*(10), 570–578. https://doi.org/10.1016/j.tins.2013.06.004
- Roch, C., Leroy, C., Nehlig, A., & Namer, I. J. (2002). Magnetic resonance imaging in the study of the lithium-pilocarpine model of temporal lobe epilepsy in adult rats. *Epilepsia*, *43*(4), 325–335. https://doi.org/10.1046/j.1528-1157.2002.11301.x
- Roger, M., & Cadusseau, J. (1985). Afferents to the zona incerta in the rat: a combined retrograde and anterograde study. *The Journal of comparative neurology*, 241(4), 480–492. https://doi.org/10.1002/cne.902410407
- Sankar, R., Shin, D. H., Liu, H., Mazarati, A., Pereira de Vasconcelos, A., & Wasterlain, C. G. (1998). Patterns of status epilepticus-induced neuronal injury during development and long-term consequences. *The Journal of neuroscience*, 18(20), 8382–8393. https://doi.org/10.1523/INEUROSCI.18-20-08382.1998
- Sankar, R., Shin, D. H., & Wasterlain, C. G. (1997). Serum neuron-specific enolase is a marker for neuronal damage following status epilepticus in the rat. *Epilepsy research*, 28(2), 129–136. https://doi.org/10.1016/ s0920-1211(97)00040-5
- Schmued, L. C., & Hopkins, K. J. (2000). Fluoro-Jade: novel fluorochromes for detecting toxicant-induced neuronal degeneration. *Toxicologic pa-thology*, 28(1), 91–99. https://doi.org/10.1177/019262330002800111
- Scholl, E. A., Dudek, F. E., & Ekstrand, J. J. (2013). Neuronal degeneration is observed in multiple regions outside the hippocampus after lithium pilocarpine-induced status epilepticus in the immature rat. *Neuroscience*, 252, 45–59. https://doi.org/10.1016/j.neuroscience.2013.07.045
- Steinert, J. R., Chernova, T., & Forsythe, I. D. (2010). Nitric oxide signaling in brain function, dysfunction, and dementia. *The Neuroscientist: a review*

- journal bringing neurobiology, neurology and psychiatry, 16(4), 435–452. https://doi.org/10.1177/1073858410366481
- Thom M. (2018). New perspectives in epilepsy neuropathology. *Neuropathology and applied neurobiology*, *44*(1), 3–5. https://doi.org/10.1111/nan.12464
- Turski, L., Diedrichs, S., Klockgether, T., Schwarz, M., Turski, W. A., Sontag, K. H., Bortolotto, Z. A., Calderazzo-Filho, L. S., & Cavalheiro, E. A. (1991). Paradoxical anticonvulsant activity of the gamma-aminobutyrate antagonist bicuculline methiodide in the rat striatum. *Synapse (New York, N.Y.)*, 7(1), 14–20. https://doi.org/10.1002/syn.890070103
- Vila Verde, D., Zimmer, T., Cattalini, A., Pereira, M. F., van Vliet, E. A., Testa, G., Gnatkovsky, V., Aronica, E., & de Curtis, M. (2021). Seizure activity and brain damage in a model of focal non-convulsive status epilepticus. *Neuropathology and applied neurobiology*, 47(5), 679–693. https:// doi.org/10.1111/nan.12693
- Wagner, C. K., Eaton, M. J., Moore, K. E., & Lookingland, K. J. (1995). Efferent projections from the region of the medial zona incerta containing A13 dopaminergic neurons: a PHA-L anterograde tract-tracing study in the rat. *Brain research*, 677(2), 229–237. https://doi.org/10.1016/0006-8993 (95)00128-d
- Wang, Q., Zhang, X., Leng, H., Luan, X., Guo, F., Sun, X., Gao, S., Liu, X., Qin, H., & Xu, L. (2020). Zona incerta projection neurons and GABAergic and GLP-1 mechanisms in the nucleus accumbens are involved in the control of gastric function and food intake. *Neuropeptides*, 80, 102018. https://doi.org/10.1016/j.npep.2020.102018
- Watson, C., Lind, C. R., & Thomas, M. G. (2014). The anatomy of the caudal zona incerta in rodents and primates. *Journal of anatomy*, 224(2), 95–107. https://doi.org/10.1111/joa.12132
- Watson, G. D., Smith, J. B., & Alloway, K. D. (2015). The Zona Incerta Regulates Communication between the Superior Colliculus and the Posteromedial Thalamus: Implications for Thalamic Interactions with the Dorsolateral Striatum. *The Journal of neuroscience: the official journal of the Society for Neuroscience*, 35(25), 9463–9476. https://doi.org/10.1523/JNEUROSCI.1606-15.2015
- Xu, H., Liu, L., Tian, Y., Wang, J., Li, J., Zheng, J., Zhao, H., He, M., Xu, T. L., Duan, S., & Xu, H. (2019). A Disinhibitory Microcircuit Mediates Conditioned Social Fear in the Prefrontal Cortex. *Neuron*, *102*(3), 668–682.e5. https://doi.org/10.1016/j.neuron.2019.02.026